




# Bond durability between anchored GFRP bar and seawater concrete under offshore environmental conditions

Hamidreza Kazemi · Mohammad Yekrangnia  · Milad Shakiba ·  
Milad Bazli · Asghar Vatani Oskouei

Received: 29 September 2022 / Accepted: 15 March 2023 / Published online: 29 March 2023  
© The Author(s) 2023

**Abstract** The lower bond strength of FRP bars to concrete compared to steel bars has remained an unsolved barrier to the widespread use of FRP-reinforced concrete under extreme loading. Additionally, the degradation of the bond between FRP reinforcement and concretes in aggressive environments adds to the existing concern. In this study, an innovative anchorage system comprised of polypropylene pipe was used to strengthen the bond between seawater concrete and GFRP bars after 250 days of exposure to offshore environmental conditions. As material factors, two types of GFRP bars (sand-coated and ribbed) and two types of concrete (normal and seawater concrete) were evaluated. Four distinct environmental conditions were used to assess the samples: (i) ambient environment (control), (ii) tap water, (iii) seawater, and (iv) wet-dry cycles in seawater. According to the findings of the direct

pull-out tests, the suggested anchor system strengthens the bond and shifts the failure mode from bond failure to bar rupture. Additionally, after exposure to 250 days of seawater wet-dry cycles, GFRP-reinforced seawater concrete lost 5% of its maximum bond strength (developed bar tensile stress). All other samples exposed to different environmental conditions either increased or decreased in bond strength by less than 5% after 250 days, compared to the control samples.

**Keywords** Bond strength · Bond durability · Offshore environment · GFRP · Seawater concrete · Wet-dry cycles · Mechanical anchorage

## 1 Introduction

The overuse of fresh water in the production of ordinary concrete has become a severe environmental problem, particularly in nations with limited access to water. Because of its availability in offshore locations, employing seawater to make concrete can significantly help alleviate freshwater scarcity [1, 2]. However, traditional carbon steel should not be utilized in conjunction with seawater due to the steel's susceptibility to corrode when subjected to chloride ions [2–5]. To overcome this issue, substituting Fibre reinforced polymer (FRP) composites as corrosion-resistant materials instead of carbon steel may be a

---

H. Kazemi · M. Yekrangnia (✉) ·  
M. Shakiba · A. Vatani Oskouei  
Department of Civil Engineering, Shahid Rajaei Teacher  
Training University, Lavizan, Tehran, Iran  
e-mail: yekrangnia@sru.ac.ir

M. Bazli (✉)  
Faculty of Science and Technology, Charles Darwin  
University, Darwin 0801, Australia  
e-mail: milad.bazli@cdu.edu.au; m.bazli@uq.edu.au

M. Bazli  
School of Mechanical and Mining Engineering, The  
University of Queensland, Brisbane, Australia



viable option [6–8]. FRP has been widely used in a variety of civil and construction applications [9–12], most notably to retrofit and/or reinforce concrete structures. Numerous reasons can be mentioned in this regard, including their appropriate mechanical characteristics with outstanding high strength/stiffness-to-weight ratio [13–15], exceptional durability in corrosive conditions [10, 16, 17] and ease of fabrication, transportation, and installation [17–19]. Composite materials, in particular, have remarkable corrosion resistance, which makes them an appealing alternative to steel in corrosive conditions, such as offshore constructions [18, 20–22].

To develop appropriate design standards, it is critical to understand the bond behaviour between the concrete and the reinforcing bar [23, 24]. However, significant disparities in bond strength exist between steel and FRP-reinforced concretes. This is attributable to a variety of factors, including material characteristics and the shape of the bar [25, 26]. The design bond strength between concrete and steel is primarily determined by concrete shear strength, whereas the design bond strength of FRP reinforced concretes is determined by both concrete shear strength and FRP bar surface failure [27]. The low shear strength and wear performance of the FRP bar has made its bond with concrete a serious concern when it comes to extreme loads. Furthermore, solution penetration into the FRP bars could lead to the degradation of their mechanical properties and consequently reduce bond strength. On the other hand, the vulnerability of such structures to corrosion when exposed to corrosive environments is known as a serious challenge to the integrity and bond performance of steel-reinforced concretes. Therefore, using corrosion-resistant FRP bars, as an alternative to carbon steel, capable of bearing significant bond stress to reinforced concrete structures subjected to corrosive environments is key. In this regard, several researchers have proposed different methods to enhance the bond performance between FRP bars and concrete. The mechanical interlocking of FRP bars and concrete is accomplished by a variety of parameters, including chemical bonding, friction, and mechanical interlocking [28–30]. To increase the mechanical interlocking and friction between FRP bar and concrete, methods such as using ribbed, helically grooved, and sand-coated bars, as well as different mechanical anchorage systems [31–38] have

been used. The common solution for steel-reinforced parts is to employ regular 90 and 180° bends in the bars. However, FRP bars cannot be bent after construction, and when constructed with hooks, the redirection of the fibres at corners greatly reduces their strength [39]. As a result, anchor plates and headed ends have been considered suitable solutions to the load transmission problem between concrete and FRP bars. Despite efforts to improve the bond between concrete and FRP bars, more work remains to be done to provide an adequate bond in FRP-reinforced concrete structures.

Although numerous studies have been conducted to study the bond performance of various concrete and FRP bars [31, 40–42], most of them have concentrated on short-term performance [43]. Indeed, some researchers have examined the durability of the bond between concrete and FRP bars subjected to various conditions, including seawater [44–48]. Some of the studies on the FRP-concrete bond durability, when subjected to environmental conditions, have been summarised in Table 1. However, very few studies have focused on concrete including seawater in its mix. Furthermore, to the best knowledge of the authors, there not no study considering the effect of the anchorage system on the bond durability of GFRP-reinforced concrete after exposure to corrosive environments.

Therefore, the significance of the present study lies in studying the bond durability of GFRP-reinforced concrete in offshore environmental conditions taking into account the effects of a sustainable anchorage system, concrete type, bar type, and conditioning environments.

## 2 Experimental program

A total number of 48 specimens were prepared and tested under direct pull-out to study the bond durability between seawater concrete and GFRP bars after 250 days of exposure to (i) ambient laboratory weather (AW), (ii) immersion in tap water (TW), (iii) immersion in seawater (SW), and (iv) wet-dry cycles in seawater (W/D).



**Table 1** Studies on FRP bar-concrete bond durability [49]

Ref	Bar type	Concrete type	Conditioning environment
[25]	BFRP, GFRP, and CFRP	Normal	Seawater
[44]	BFRP	Fibre-reinforced	Seawater
[45]	BFRP and steel	Seawater sea sand	Seawater and wet-dry cycles
[46]	BFRP	Normal and fly ash	Alkaline and seawater solutions
[50]	GFRP	Normal	water and air thermal cycles
[51]	GFRP	Normal	Water
[52]	GFRP	Normal	Seawater
[53]	BFRP	Normal	Alkaline solution
[54]	GFRP and BFRP	Normal	Seawater and tap water
[55]	GFRP and BFRP	Normal	Seawater, acidic, and alkaline solutions
[56]	BFRP	Normal	Seawater
[57]	GFRP	Fibre-reinforced	Seawater
[58]	GFRP and CFRP	Fibre-reinforced	Deicing salt solution + freeze-thaw cycles
[59]	GFRP	Normal	Alkaline-saline solution + Freeze-thaw cycles
[60]	BFRP	Normal and fibre reinforced	seawater
[61, 62]	GFRP	Normal	Water and acidic solutions
[63]	GFRP and CFRP	Coral	Seawater
[64]	GFRP (ribbed)	Normal, self-compacting, high-strength, and light-weight	Seawater, alkaline, and acidic Solutions and wet-dry cycles

## 2.1 Materials

### 2.1.1 GFRP bars

Two types of 8 mm GFRP bars, namely (i) sand-coated (SG) and ribbed (RG), made of E-glass-fibres and epoxy resin were used (Fig. 1). According to the manufacturer, both bars were constructed using 80%



**Fig. 1** GFRP bars: **a** sand coated, **b** Ribbed

fibre to 20% resin and additives volumetric ratio. The mechanical properties of GFRP bars are presented in Table 2.

### 2.1.2 Concretes

Type II Portland cement with a specific surface of  $3050 \text{ cm}^2/\text{gr}$  was used. Two types of concrete, namely normal concrete (NC) and seawater concrete (SWC) were considered. Seawater was used in SWC, while freshwater was used in NC. Natural river gravel of 19 mm maximum size and natural river sand of 3.0 fineness modulus were used. Eighteen standard concrete cylinders were constructed and tested under compression and Brazilian tensile test according to ASTM C39 [14], and ASTM C496 [65]. For each concrete, three identical specimens were tested after (i) 28 days of curing based on ACI 308R recommendation [66] and (ii) 250 days of conditioning in each environmental condition. The strength results used in the discussion are the averages of three identical specimens for each concrete. Tables 3 and 4 illustrate

**Table 2** Mechanical characteristics of GFRP bars according to the manufacturer

Type of bar	Diameter (mm)	Density (gr/cm <sup>3</sup> )	Elastic modulus (GPa)	Tensile strength (MPa)	Thermal conductivity (W/mK)
SG	2.20	8	55	1024	0.50
RG	2.20	8	50	950	0.50

**Table 3** Mix design composition

Concrete type	Water type	W/C	Cement (kg/m <sup>3</sup> )	Water (kg/m <sup>3</sup> )	Gravel (kg/m <sup>3</sup> )	Sand (kg/m <sup>3</sup> )	Slump (mm)
NC	Freshwater	0.4	400	160	1178	795	61
SWC	Seawater	0.4	400	160	1178	795	59

**Table 4** Strength results of concretes

Concrete Type	Compressive strength (MPa) (COV%)	After 28 days of curing Tensile strength (MPa) (COV%)	After 250 days of conditioning			
			Compressive strength (MPa)			
			AW (COV%)	TW (COV%)	SW (COV%)	W/D (COV%)
NC	27.43 (0.8%)	2.87 (1.3%)	28.64 (2.1%)	29.17 (1.1%)	26.38 (1.7%)	25.33 (2.6%)
SWC	20.87 (1.1%)	2.31 (2.2%)	23.18 (1.6%)	23.69 (2.5%)	23.09 (0.7%)	21.48 (0.9%)

**Table 5** Material properties of the adhesive

Type of adhesive	Density (gr/cm <sup>3</sup> )	After 7 days			
		Adhesion strength (MPa)	Compressive strength (MPa)	Tensile strength (MPa)	Flexural strength (MPa)
ABABOND RA-500	1.40	16	100	20	40

the mix design of the concretes and the strengths after 28 and 250 days of conditioning, respectively.

## 2.2 Specimens

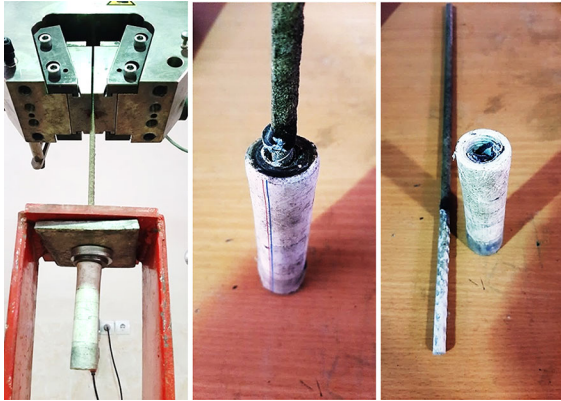
In this study an innovative anchorage system made of polypropylene pipe filled with high-strength adhesive, ABABOND RA 500 has been used. Based on the provider's technical sheets, Tables 5 and 6 list the material properties of the polypropylene pipe and the adhesive used, respectively. The internal surface of the pipes was machine-grooved to increase its bond with the glue. The optimised anchorage length was obtained after conducting the pull-out test on the GFRP bar embedded in the anchorage system (Fig. 2). This was done to make sure that there would be no bar

slippage from the anchorage system before the bar rupture. In this case, the ultimate tensile strength of the GFRP bar could be achieved during the bond pull-out test. According to the test results, pipes with a length of 160 mm, an outer diameter of 25 mm and an inner diameter of 18 mm were selected as the optimised system. Figures 3 and 4 show the proposed anchorage system configuration and the bar placed inside the anchorage pipe. According to ACI 440. 3R [67], a minimum embedment length equal to 5 times the bar diameter is generally considered for the direct pull-out test of GFRP bars without a mechanical anchorage system. It should be noted that the anchorage length (160 mm) itself is longer than 40 mm (5 times 8 mm). Anchored GFRP bars were embedded in 150 × 300 mm cylindrical concrete members. It



**Table 6** Material properties of the polypropylene pipe

Type of pipe	Density (gr/cm <sup>3</sup> )	Size (mm)	Outer diameter (mm)	Inner diameter (mm)	Wall Thickness (mm)	Flexural strength (MPa)	Tensile testing		
							Yield Strain	Yield strength (MPa)	Ultimate strength (MPa)
PP-RC	0.91	19	25	18	3.5	16.4	0.125	25.8	33.6

**Fig. 2** Pull-out test set-up and failure mode for GFRP bar in the anchorage system

should be noted that both ends of GFRP bars inside the concrete were deboned and sealed by 10 mm PVC tubes to avoid end effects and solution penetration in the longitudinal direction. Moreover, to prevent premature bar failure inside the testing machine grip, GFRP bars were placed inside steel tubes which were both internally and externally grooved (Fig. 5). High-strength epoxy resin was used to fill the steel tubes. Following the pouring of concrete into moulds, samples were put on a vibration table and vibrated to obtain the desired compaction level. After 24 h, specimens were taken from the moulds and cured for 28 days in tap water and seawater before being exposed to different environments.

One of the advantages of the proposed anchorage system in actual applications is that one or multiple anchors can be used in any location along the bar length. The total length and the number of anchors used can be optimised based on the required bar stress ratio according to the design guideline used. The results of the present study could be used to understand the obtained bar stress ratio in case a single 160 mm anchor is used for a concrete compressive strength

ranging from 21 to 30 MPa and a concrete cover of 75 mm. However, further study is needed to investigate the efficiency of the anchorage system in terms of the anchorage diameter, anchorage length, number of anchors and the space between the anchors in case of using more than one anchor. Figure 6 shows the bar location embedded in concrete as well as the bond configuration.

### 2.3 Environmental conditioning

To investigate the bond performance between GFRP bars and SWC or NC, specimens were subjected to 250 days under laboratory simulated circumstances. Simulated environments, including (i) laboratory ambient weather (AW) at 25 °C, (ii) immersion in tap water (TW) at 25 °C, (iii) immersion in seawater immersion (SW) at 25 °C, and (iv) wet-dry cycles in seawater(W/D) 25 °C for 250 days (i.e. 500 cycles). In the W/D condition, for 24 h of a day, samples were immersed in seawater for 12 h followed by 12 h in a dry environment at ambient temperature. Seawater was manufactured in such a way that it resembled the chemical composition of Persian Gulf water for the SW and W/D conditions. The chemical compositions utilised were 27.50 (gr/lit) NaCl, 5.10 (gr/lit) MgCl<sub>2</sub>, 1.11 CaCl<sub>2</sub> (gr/lit), 0.76 (gr/lit) KCl, and 0.1 (gr/lit) KBr. It is worth mentioning that in all immersion conditioning, specimens were immersed up to the concrete level to make sure that the bare length of GFRP bars are not in contact with the solution.

### 2.4 Direct pull-out test

Direct pull-out tests were carried out using a Universal Testing Machine Zwick Roell servo-electric universal testing machine equipped with a 150 kN load cell. To capture the samples' post-peak behaviour, a displacement-controlled loading regime with a constant rate of

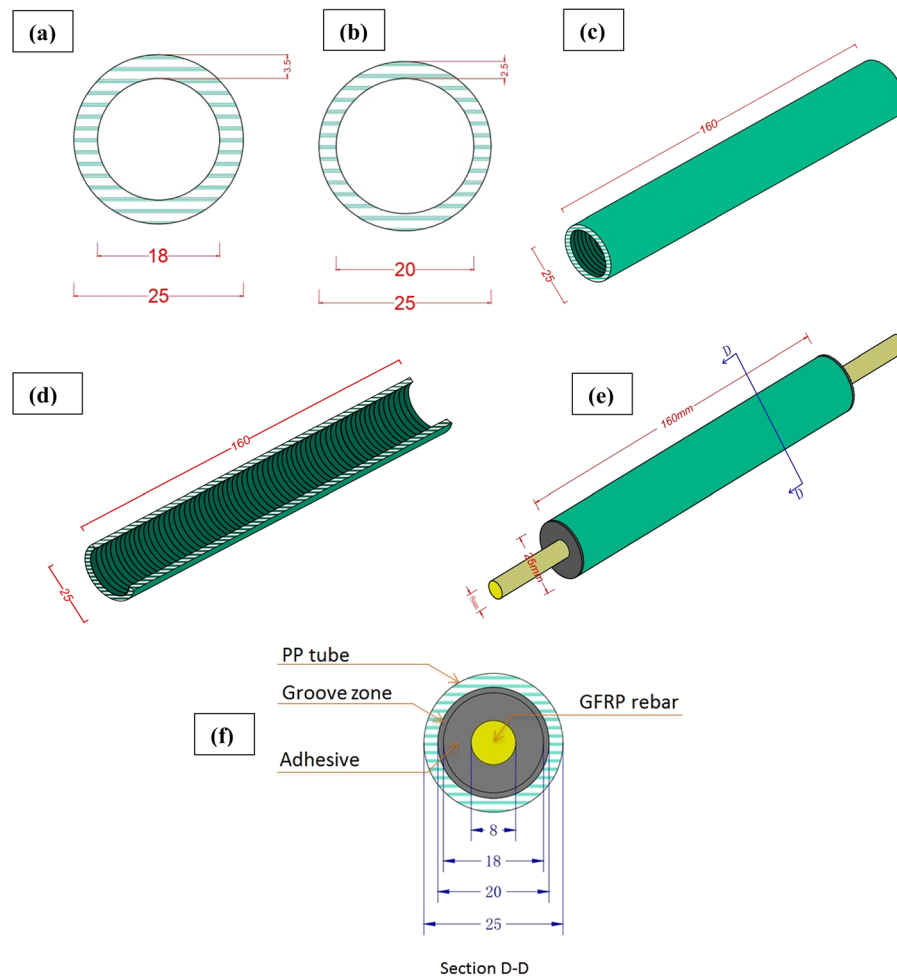


**Fig. 3** Schematic drawing of the anchorage system configuration (units are in mm): **a** PP pipe cross-section before inner grooving, **b** PP pipe cross-section after inner grooving,

**c** Grooved PP pipe, **d** interior view of the grooved PP pipe, **e** final view of an anchorage system, and **f** anchor cross-section

1.2 mm/min was applied to all samples. Throughout the test, linear variable differential transformers (LVDTs) were employed to continually record the bar slip values. The pull-out test setup employed in this study is depicted in Fig. 7.

### 3 Results and discussion

#### 3.1 Failure modes

In the present study, anchored GFRP bars embedded in concrete have shown two different failure modes.

Samples made of normal concrete and exposed to AW and TW conditions (25% of the total specimens) failed due to the GFRP bar rupture, while all other samples failed in pull-out failure mode (i.e. bond failure with no sign of concrete splitting). As mentioned earlier, the length of the anchorage system was optimised in order to achieve GFRP bar rupture failure rather than bar slippage from the pipe. Bar rupture failure observed in normal concrete control samples shows that the bond strength between the concrete and the anchorage system was also adequate so that the ultimate tensile capacity of the bar was achieved. As expected, due to the insignificant bond performance variations and an increase in concrete



**Fig. 4** Actual anchored bars: **a** prepared pipes, and **b** GFRP bars placed inside the pipes



**Fig. 5** Grooved steel pipe used for testing GFRP bars

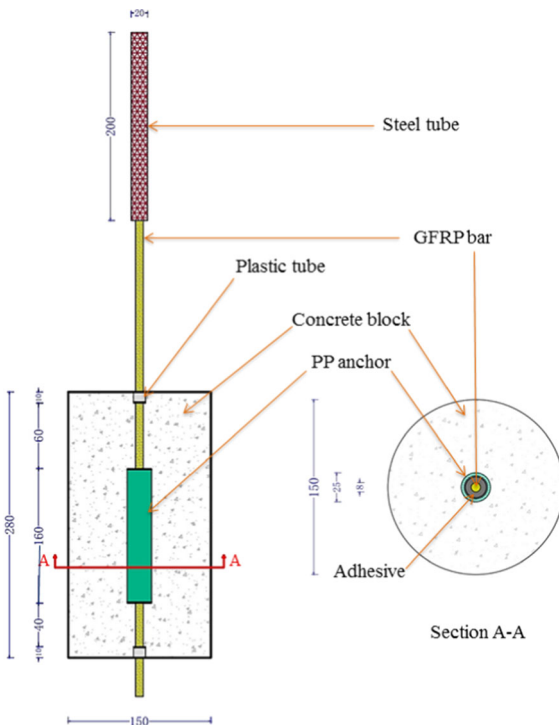


**Fig. 6** Dimensions and configurations of the specimen (units are in mm)

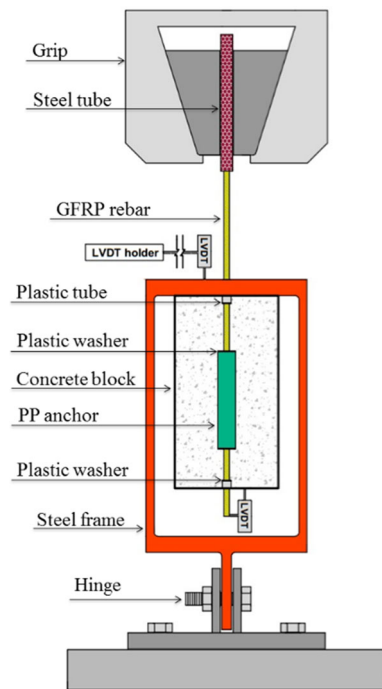


**Fig. 7** Direct pull-out test set-up

compressive strength due to ageing in AW and TW environments, the failure mode did not change. However, in specimens made of seawater and those exposed to seawater environments, the bond degradation overcomes the concrete curing effect, and thus changes the failure mode from the bar rupture to the pull-out failure. The pull-out failure in all samples was related to GFRP bar surface failure (bar surface peeling-off).

Visual inspection of the interface between the concrete and the bar revealed that failure occurs between the sand coat and the bar surface resin layer in specimens reinforced with sand-coated GFRP bars (SG), whereas specimens reinforced with ribbed bar (RG) experienced a bond failure between the concrete and the bar interface. This could be because the silica sand used to cover the GFRP bar forms a strong chemical bond with the concrete. It is well established that silica sand absorbs huge amounts of  $\text{OH}^-$  and  $\text{Ca}^{++}$  from the cement solution while also releasing significant amounts of  $\text{Si}^{4+}$  in the cement paste.  $\text{Ca}^{++}$  and  $\text{OH}^-$  are absorbed by silica sand, resulting in the creation of hydrated silicates. Due to the greater surface area exposed, this chemical reaction is more pronounced in finer sand [68].

It is worth mentioning that no sign of bar slippage from the anchorage pipe was observed in any of the

samples. This confirms the efficiency of the proposed anchorage system under corrosive environments. Figure 8 shows typical failure modes of both bar rupture and pull-out failure modes observed in this study.

### 3.2 Bond performance

The pullout load–displacement and load-slip curves of each specimen are depicted in Figs. 9 and 10, respectively. A linear relationship between the values of the pullout load and the associated displacement is expected in a case of appropriate bond performance between the concrete and the anchor (such behaviour was observed in all samples before reaching the maximum bond strength). Indeed, the presence of longitudinal and surface cracks weakens the bond between the concrete and the anchor.

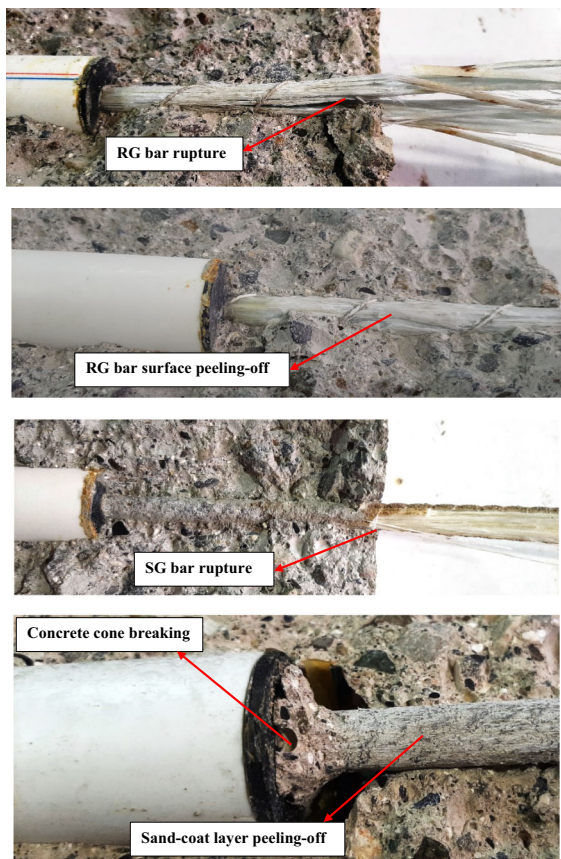


**Fig. 8** Typical failure modes of both bar rupture and pull-out failure modes of RG and SG specimens



As is seen in Fig. 9, RG bar specimens subjected to SW or W/D showed slight stiffness (i.e. slope of load–displacement curves) reductions despite those of the corresponding SG bar specimens. Such difference could be explained by different failure modes observed between RG and SG reinforced specimens. As mentioned earlier, the strong chemical bond between the concrete and the sand coat results in the failure to occur at the interface between the GFRP bar surface resin and the sand coat (see Fig. 8). Therefore, based on the observed results, one could conclude that this interface is less vulnerable to aggressive solutions than that of RG bar and concrete interface. This could be because the GFRP bar surface resin and the sand coat interface is an inner layer while the interface between RG bar and concrete is the exterior layer of GFRP bars. In other words, the layer is directly exposed to aggressive solutions.

Apart from some stiffness degradation of RG-reinforced concrete exposed to seawater environments, all other samples showed negligible changes in their stiffness property. This confirms that the elastic modulus of GFRP reinforcement is not significantly affected by seawater. A similar conclusion has been reported by other researchers [17].

There are three primary mechanisms by which the bond strength between concrete and FRP is transferred: chemical bond, mechanical interlocking and friction. Numerous factors influence how much each mechanism contributes to the bond strength. Reinforcement bar type, shear strength, surface configuration, elastic modulus, and type of concrete and its strength are some of these parameters [69]. The extent of damage caused by exposure to harsh environments is dependent on a variety of parameters, including the exposure condition, temperature, duration, the type of fibre and resin used, their chemical composition, and the type and permeability of the concrete. Not only does damage to the bar alter its mechanical properties, but it also weakens its bond with the concrete [68]. Once the GFRP bar degradation process begins, the degradation agents tend to degrade and weaken the matrix and resin/fibre interface. In case of exposure to seawater, hydroxyl ions may cause chemical interactions with other ions such as  $\text{Na}^+$ . Additionally, seawater may induce blisters on the surface of the bars, resulting in resin deformation and hence a reduction in bond strength [70].



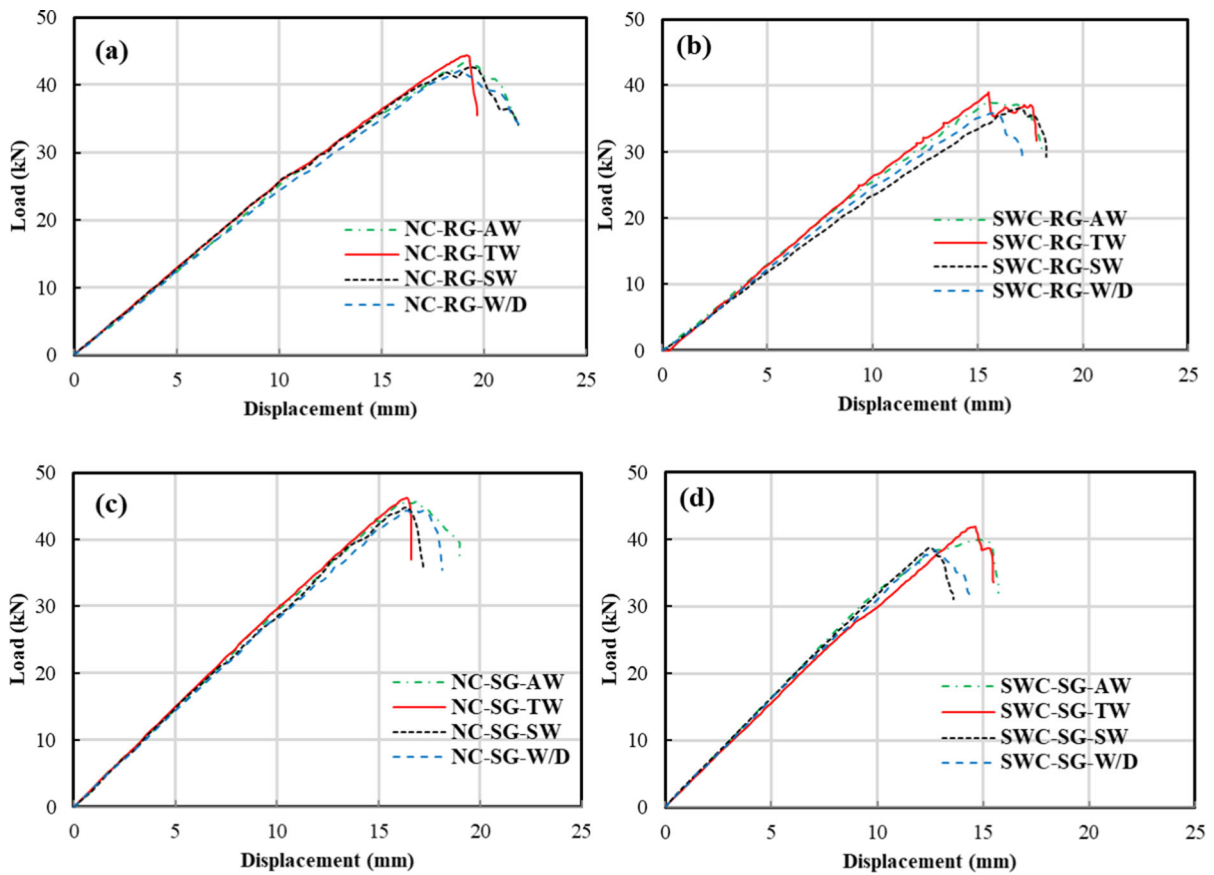


**Fig. 9** Load–displacement curves of representative specimens

The following sections will explore in-depth the effect of environmental variables on the bond performance of anchored GFRP bars and seawater/normal concrete.

### 3.2.1 Developed tensile stress

Due to the presence of the anchorage system, calculating the average bond strength is not feasible. Thus, the ratio between the developed tensile stress ( $f_s$ ) in the GFRP bar and the nominal tensile strength of the bar,  $f_{ps}$  is used to compare the bond performance of different specimens. Therefore, in the present study, bond strength is represented by the developed tensile stress. Tensile stress in GFRP bars is calculated by dividing the applied pullout force applied to the bar by its nominal cross-section. Table 7 summarises the maximum applied load, developed tensile stress and  $f_s/f_{ps}$  ratios of tested specimens under pull-out  $f_s/f_{ps}$  ratio values close to 1, confirming that the presence of the

proposed anchor provides an appropriate mechanical interlocking along with the specimen.

In this section, the effect of concrete type, type of GFRP bar, and conditioning environment on  $f_s/f_{ps}$  ratios will be investigated.

**3.2.1.1 Effect of bar type** As can be seen in Fig. 9, regardless of the concrete type and the exposure condition, the SG bars show a load, corresponding to the initial slip of the anchorage system in the concrete, higher with respect to RG bars for both types of concrete NC and SWG. This is due to the strong chemical bond formation between the sand coat layer and the concrete during the conditioning process.

Figure 11 compares the developed tensile stress ratios of GFRP-reinforced samples exposed to aggressive environments with respect to the GFRP bar type. Three phenomena have effects on the bond strength and bond durability when subjected to environmental conditions containing moisture: (1) change in the

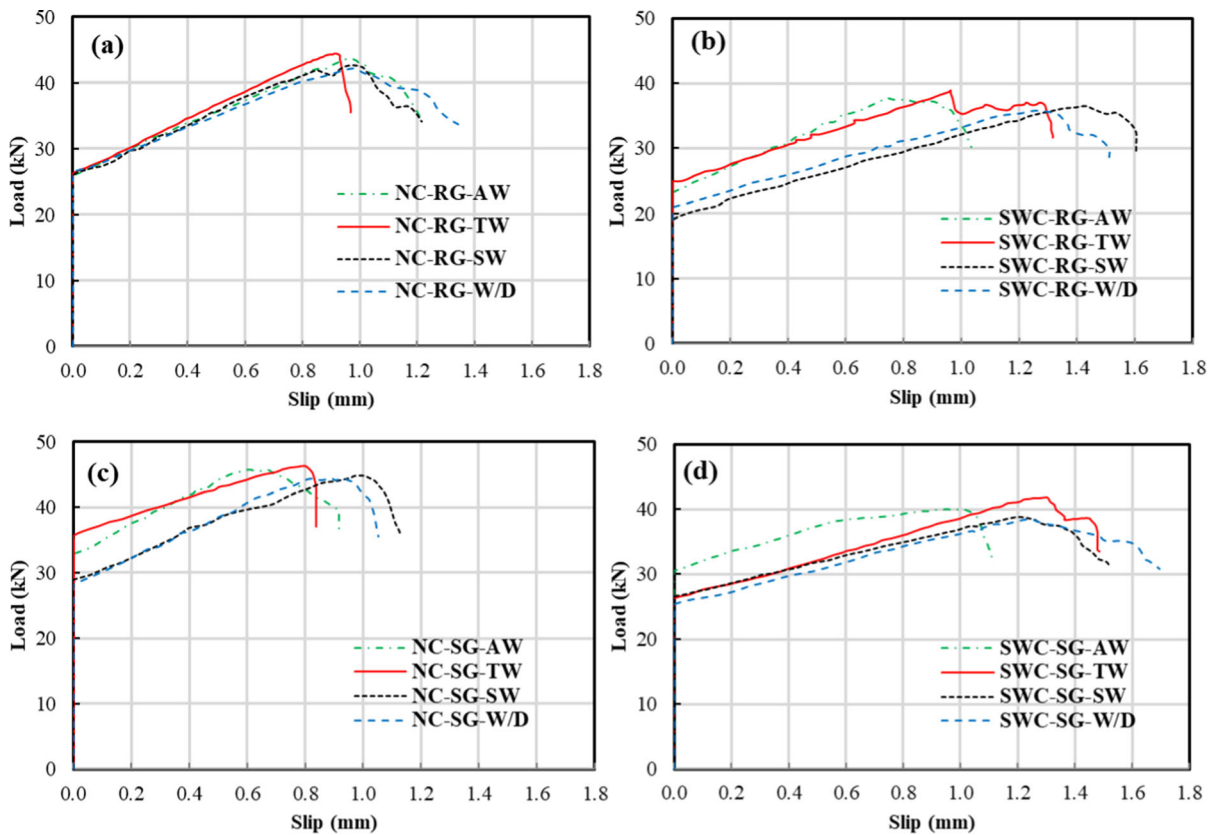


**Fig. 10** Load-slip curves of representative specimens

**Table 7** Pull-out test results

Specimen	Average load (kN)	CoV (%)	$f_s$	$f_s/f_{ps}$	Failure mode
NC-RG-AW	43.68	0.20	869.45	0.92	Bar rupture
NC-RG-TW	44.37	1.41	883.12	0.93	Bar rupture
NC-RG-SW	42.63	2.10	848.59	0.89	Bond failure
NC-RG-W/D	42.20	2.31	840.01	0.88	Bond failure
NC-SG-AW	45.70	0.79	909.63	0.89	Bar rupture
NC-SG-TW	46.32	2.40	921.99	0.90	Bar rupture
NC-SG-SW	44.74	0.51	890.51	0.87	Bond failure
NC-SG-W/D	44.37	0.64	883.14	0.86	Bond failure
SWC-RG-AW	37.68	4.18	749.98	0.79	Bond failure
SWC-RG-TW	39.01	2.72	776.39	0.82	Bond failure
SWC-RG-SW	36.49	3.91	726.39	0.76	Bond failure
SWC-RG-W/D	35.83	4.03	713.24	0.75	Bond failure
SWC-SG-AW	39.99	3.82	795.96	0.78	Bond failure
SWC-SG-TW	41.87	4.80	833.44	0.81	Bond failure
SWC-SG-SW	38.81	4.04	772.47	0.75	Bond failure
SWC-SG-W/D	38.46	6.30	765.53	0.75	Bond failure

compressive strength of concrete due to curing. If correctly cured, this could result in a significant increase in bond strength; (2) FRP bar expansion owing to solution diffusion. This raises the bond strength because of an increase in the mechanical interlocking between the concrete and the bar; (3) Chemical interactions between the solution, fibre, concrete, and resin (i.e. sulphate and chloride reactions). This is a disadvantage of seawater conditioning [54]. The main difference between the specimens reinforced with sand-coated GFRP and ribbed GFRP when subjected to environmental conditions will be the chemical reactions (number 3). This was also observed in failure modes between the two types (see Fig. 11).

It is seen that regardless of the concrete type and the exposure condition compared to their corresponding control samples, sand-coated GFRP specimens show slightly better bond performance (i.e. less degradation compared to their corresponding control samples) in all conditions. For example, NC-RG-AW has a stress ratio of 0.92 as a control sample for the RG bar and NC-RG-W/D has a ratio of 0.88 as a conditioned sample for the RG bar. Therefore, a 4.3% reduction has occurred for this condition compared to the reference sample. Similarly, NC-SG-AW has a stress ratio of 0.89 as a control sample for the SG bar and NC-SG-W/D has a ratio of 0.86 as a conditioned sample for the SG bar. Therefore, a 3.3% reduction has occurred for this condition compared to the reference sample. As mentioned earlier, this is due to the strong

chemical bond between the sand coat layer and the concrete. In other words, the degradation between the sand coat and bar surface resin in the SG specimen is somewhat lower than the degradation between the bar surface and concrete in the RG specimens.

**3.2.1.2 Effect of the concrete type** Figure 12 compares the developed tensile stress ratios of GFRP-reinforced samples exposed to aggressive environments with respect to the concrete type. As expected, independent of the bar type, the stress ratios of NC specimens subjected to seawater or subjected to wet-dry cycles in seawater were higher than those of SWC specimens. Different compressive strengths of concrete and their fluctuation after conditioning can be the cause of this disparity. When concrete is subjected to seawater, chloride ions chemically react with the cement mass, eventually neutralising it (reducing the alkalinity of the cement paste). This speeds up the leaching of portlandite and hence increases the porosity of the concrete. This eventually results in the deterioration of the concrete's strength and stiffness [71]. As mentioned earlier, GFRP bar swelling and concrete curing may increase the bond strength of specimens exposed to moisture. Both SWC and NC specimens exposed to W/D showed lower stress ratios compared with the control specimens (i.e. specimens exposed to AW). However, the ratios of conditioned SWC samples compared to the SWC control sample were comparable with the ratios of conditioned NC samples compared with the NC

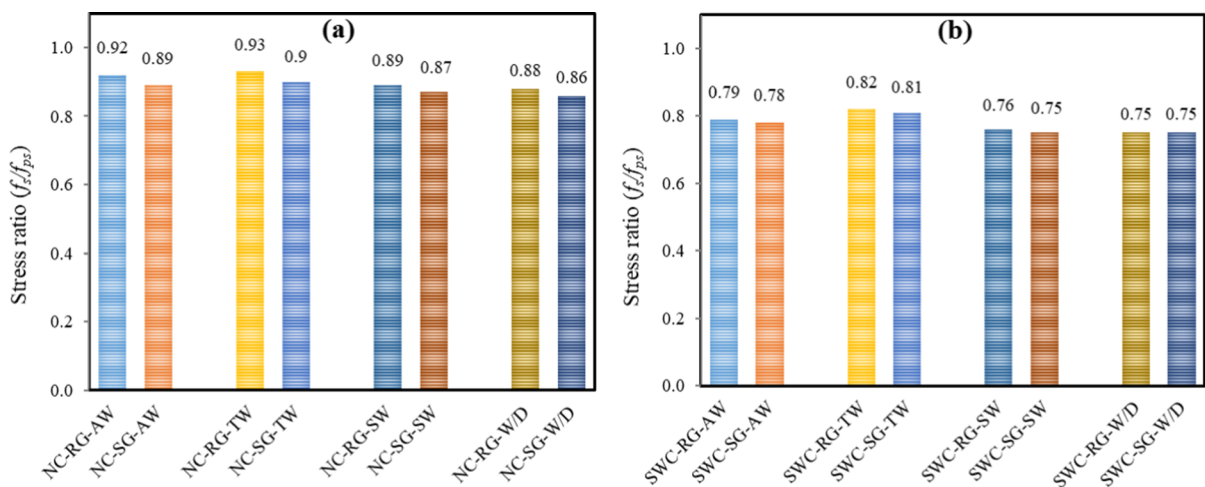


**Fig. 11** Developed tensile stress ratios with respect to the type of GFRP bar: **a** NC and **b** SWC

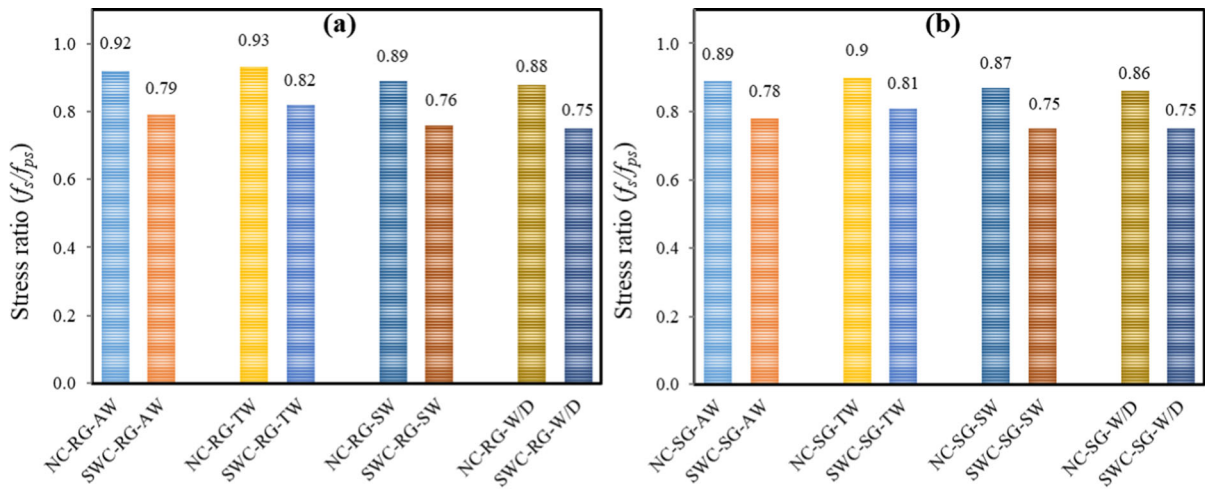


**Fig. 12** Developed tensile stress ratios with respect to the concrete type: **a** RG and **b** SG

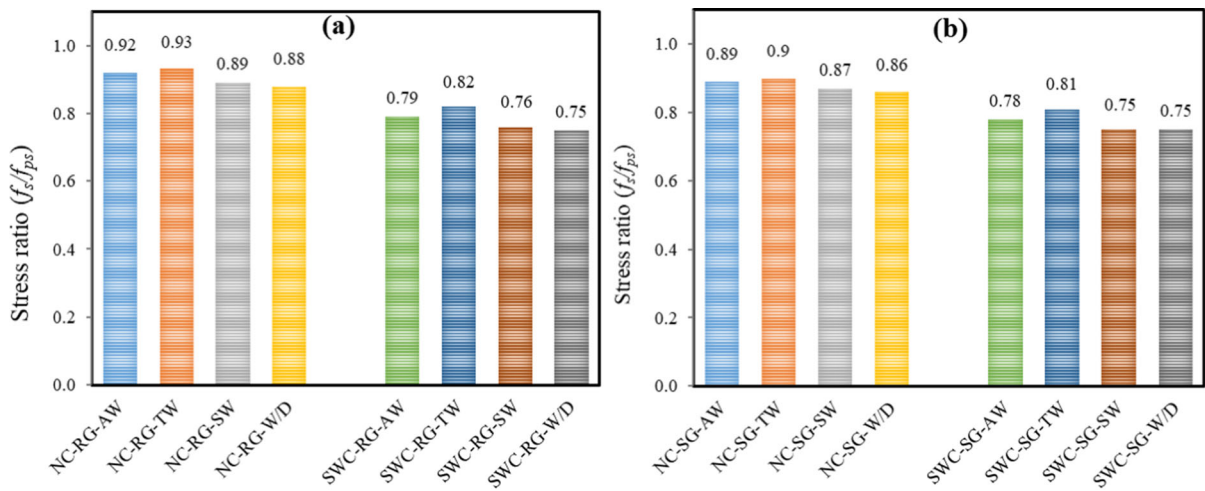


**Fig. 13** Developed tensile stress ratios with respect to the conditioning type: **a** RG and **b** SG

control sample. This could be due to the slightly higher compressive strength gain of SWC compared with NC after 250 days of curing in TW compared with AW (see Table 4). The results reported by Mohammed et al. [72] also confirm that SWC shows faster strength gain compared with NC.

**3.2.1.3 Effect of conditioning type** Figure 13 compares the developed tensile stress ratios of GFRP-reinforced samples exposed to aggressive environments with respect to the conditioning environment. From Fig. 13, one can conclude that seawater W/D is the most aggressive environment, while TW is the least aggressive condition. SW

environment is somewhere between the two. It is well established that solution diffusion increases the unit volume of GFRP bars by forming microcracks. This weakens the adhesion between the resin and the fibres at their interface, resulting in the loss of the mechanical properties and the bond of GFRP bars [73]. Additionally, in seawater, hydroxyl ions are formed on glass fibres reacting with seawater components, such as sodium ions, to restore the electrical balance. Eventually, blister growth on the GFRP surface may deform the resin matrix, hence deteriorating the composite's mechanical properties [74]. It is worth noting that the thermal expansion coefficient difference between the resin and glass

fibres is the primary cause of resin degradation, and thus of bond strength and stiffness degradation [7]. On the other hand, bar swelling due to the moisture penetration, may increase the mechanical interlocking between the GFRP bar and the concrete and thus increase the bond strength. Less moisture penetration during W/D cycles compared to SW condition could be the possible reason for the higher stress ratio of specimens exposed to W/D condition in comparison to specimens exposed to SW.

#### 4 Conclusion

The bonding behaviour and durability of FRP-reinforced concrete are currently being studied by several researchers. Accordingly, this research focuses on the bond performance of GFRP bars with an innovative anchorage system embedded in seawater and normal concrete after exposure to corrosive environments. The following findings can be taken from the experimental investigation:

- (1) Innovative proposed anchorage system made of polypropylene pipe filled with high-strength adhesive significantly enhances the bond performance between GFRP bar and normal-strength concrete in a way that the ultimate tensile stress of the GFRP bar is achieved in the pull-out test.
- (2) Maximum bond strength (developed tensile stress in GFRP bars) reductions of about 5% were obtained for GFRP reinforced seawater concrete after 250 days of conditioning in seawater wet-dry cycles while other specimens immersed in tap water and seawater experienced an increase or less than 5% decrease in bond strength after 250 days.
- (3) Pull-out specimens reinforced with sand-coated GFRP bars show slightly better bond behaviour than that of specimens reinforced with ribbed GFRP bars after exposure to environmental conditions. This is due to the strong chemical bond formation between the sand coat layer and the concrete.
- (4) Specimens subjected to seawater wet-dry cycles and immersed in seawater show bond strength reduction while specimens subject to tap water show bond strength increase compared with specimens conditioned in ambient weather. The reason is the contribution of positive factors (i.e. concrete curing and bar swelling) versus the negative factor (degradation of concrete and GFRP bar in aggressive environments).
- (5) The bond durability performance of specimens made of normal concrete is generally better than that of specimens made of seawater concrete. Different concrete compressive strength and its variation after conditioning is the possible reason for this difference.

**Acknowledgements** The support of the Structural Laboratory at the Shahid Rajaei Teacher Training University is appreciated.

**Funding** Open Access funding enabled and organized by CAUL and its Member Institutions.

#### Declarations

**Conflict of interests** The authors declare that they have no known competing financial interests or personal relationships that could have appeared to influence the work reported in this paper.

**Open Access** This article is licensed under a Creative Commons Attribution 4.0 International License, which permits use, sharing, adaptation, distribution and reproduction in any medium or format, as long as you give appropriate credit to the original author(s) and the source, provide a link to the Creative Commons licence, and indicate if changes were made. The images or other third party material in this article are included in the article's Creative Commons licence, unless indicated otherwise in a credit line to the material. If material is not included in the article's Creative Commons licence and your intended use is not permitted by statutory regulation or exceeds the permitted use, you will need to obtain permission directly from the copyright holder. To view a copy of this licence, visit <http://creativecommons.org/licenses/by/4.0/>.

#### References

1. Wang Z, Zhao X-L, Xian G, Wu G, Raman RS, Al-Saadi S, Haque A (2017) Long-term durability of basalt-and glass-fibre reinforced polymer (BFRP/GFRP) bars in seawater and sea sand concrete environment. *Constr Build Mater* 139:467–489
2. Wang Z, Zhao X-L, Xian G, Wu G, Raman RS, Al-Saadi S (2017) Durability study on interlaminar shear behaviour of basalt-, glass-and carbon-fibre reinforced polymer (B/G/CFRP) bars in seawater sea sand concrete environment. *Constr Build Mater* 156:985–1004
3. Shakiba M, Bazli M, Karamloo M, Mortazavi SMR (2022) Bond-slip performance of GFRP and steel reinforced beams



- under wet-dry and freeze-thaw cycles: The effect of concrete type. *Constr Build Mater* 342:127916
4. Shekarchi M, Shakiba M, Yekrangnia M, Tannert T (2022) Performance of glued-in rod timber joints under seawater and UV exposure cycles. *Constr Build Mater* 322:126418
  5. Kaushik S, Islam S (1995) Suitability of sea water for mixing structural concrete exposed to a marine environment. *Cement Concr Compos* 17(3):177–185
  6. Li Y, Zhao X, Singh RR, Al-Saadi S (2016) Experimental study on seawater and sea sand concrete filled GFRP and stainless steel tubular stub columns. *Thin-Walled Struct* 106:390–406
  7. Bazli M, Ashrafi H, Jafari A, Zhao X-L, Raman R, Bai Y (2019) Effect of fibers configuration and thickness on tensile behavior of GFRP laminates exposed to harsh environment. *Polymers* 11(9):1401
  8. Shekarchi M, Yekrangnia M, Biniaz A, Raftery GM (2021) Effect of elevated temperatures on the compressive behavior of timber filled steel and pultruded GFRP tubes. *Compos Struct* 271:114135
  9. Oskouei AV, Bazli M, Ashrafi H, Imani M (2018) Flexural and web crippling properties of GFRP pultruded profiles subjected to wetting and drying cycles in different sea water conditions. *Polym Test* 69:417–430
  10. Wang Z, Zhao X-L, Xian G, Wu G, Raman RKS, Al-Saadi S (2018) Effect of sustained load and seawater and sea sand concrete environment on durability of basalt- and glass-fibre reinforced polymer (B/GFRP) bars. *Corros Sci* 138:200–218
  11. Ozbakkaloglu T, Akin E (2012) Behavior of FRP-confined normal-and high-strength concrete under cyclic axial compression. *J Compos Constr* 16(4):451–463
  12. Doostmohamadi A, Karamloo M, Oskouei AV, Shakiba M, Kheyroddin A (2022) Enhancement of punching strength in GFRP reinforced single footings by means of handmade GFRP shear bands. *Eng Struct* 262:114349
  13. Lam L, Teng J, Cheung C, Xiao Y (2006) FRP-confined concrete under axial cyclic compression. *Cement Concr Compos* 28(10):949–958
  14. Wang Z, Zhao X-L, Xian G, Wu G, Raman RS, Al-Saadi S (2018) Effect of sustained load and seawater and sea sand concrete environment on durability of basalt-and glass-fibre reinforced polymer (B/GFRP) bars. *Corros Sci* 138:200–218
  15. Hosseini SM, Shakiba M, Bazli M, Javaheri A (2022) Using four-point flexure test to investigate effects of temperature and bar size on the tensile properties of GFRP bars. *Polym Test* 112:107627
  16. Bazli M, Zhao X-L, Jafari A, Ashrafi H, Raman RS, Bai Y, Khezzadeh H (2021) Durability of glass-fibre-reinforced polymer composites under seawater and sea-sand concrete coupled with harsh outdoor environments. *Adv Struct Eng* 24(6):1090–1109
  17. Bazli M, Li Y-L, Zhao X-L, Raman RS, Bai Y, Al-Saadi S, Haque A (2020) Durability of seawater and sea sand concrete filled filament wound FRP tubes under seawater environments. *Compos B Eng* 202:108409
  18. Bazli M, Zhao X-L, Jafari A, Ashrafi H, Bai Y, Raman RS, Khezzadeh H (2020) Mechanical properties of pultruded GFRP profiles under seawater sea sand concrete environment coupled with UV radiation and moisture. *Constr Build Mater* 258:120369
  19. Hosseini SM, Yekrangnia M, Oskouei AV (2022) Effect of spiral transverse bars on structural behavior of concrete shear walls reinforced with GFRP bars. *J Build Eng* 55:104706
  20. Jafari A, Oskouei AV, Bazli M, Ghahri R (2018) Effect of the FRP sheet's arrays and NSM FRP bars on in-plane behavior of URM walls. *J Build Eng* 20:679–695
  21. Bazli M, Zhao X-L, Bai Y, Raman RS, Al-Saadi S (2019) Bond-slip behaviour between FRP tubes and seawater sea sand concrete. *Eng Struct* 197:109421
  22. Shekarchi M, Farahani EM, Yekrangnia M, Ozbakkaloglu T (2020) Mechanical strength of CFRP and GFRP composites filled with APP fire retardant powder exposed to elevated temperature. *Fire Saf J* 115:103178
  23. Yan F, Lin Z, Yang M (2016) Bond mechanism and bond strength of GFRP bars to concrete: a review. *Compos B Eng* 98:56–69
  24. Vilanova I, Baena M, Torres L, Barris C (2015) Experimental study of bond-slip of GFRP bars in concrete under sustained loads. *Compos B Eng* 74:42–52
  25. Dong Z, Wu G, Xu B, Wang X, Taerwe L (2016) Bond durability of BFRP bars embedded in concrete under seawater conditions and the long-term bond strength prediction. *Mater Des* 92:552–562
  26. Won J-P, Park C-G, Kim H-H, Lee S-W, Jang C-I (2008) Effect of fibers on the bonds between FRP reinforcing bars and high-strength concrete. *Compos B Eng* 39(5):747–755
  27. Achillides Z, Pilakoutas K (2004) Bond behavior of fiber reinforced polymer bars under direct pullout conditions. *J Compos Constr* 8(2):173–181
  28. Pecce M, Manfredi G, Realfonzo R, Cosenza E (2001) Experimental and analytical evaluation of bond properties of GFRP bars. *J Mater Civ Eng* 13(4):282–290
  29. Zou R, Liu F, Xiong Z, He S, Li L, Wei W (2021) Experimental study on fatigue bond behaviour between basalt fibre-reinforced polymer bars and recycled aggregate concrete. *Constr Build Mater* 270:121399
  30. Xiong Z, Zeng Y, Li L, Kwan A, He S (2021) Experimental study on the effects of glass fibres and expansive agent on the bond behaviour of glass/basalt FRP bars in seawater sea-sand concrete. *Constr Build Mater* 274:122100
  31. Zhang B, Zhu H, Wu G, Wang Q, Li T (2020) Improvement of bond performance between concrete and CFRP bars with optimized additional aluminum ribs anchorage. *Constr Build Mater* 241:118012
  32. Benmokrane B, Mohamed HM, Manalo A, Cousin P (2017) Evaluation of physical and durability characteristics of new headed glass fiber-reinforced polymer bars for concrete structures. *J Compos Constr* 21(2):04016081
  33. Maranan GB, Manalo AC, Karunasena W, Benmokrane B (2015) Pullout behaviour of GFRP bars with anchor head in geopolymer concrete. *Compos Struct* 132:1113–1121
  34. H. Khederzadeh, K. Sennah (2013) Pullout strength of pre-installed GFRP bars in concrete. In: CSCE 2013 general conference. quebec, Canada2013, pp 1–9
  35. Islam S, Afefy HM, Sennah K, Azimi H (2015) Bond characteristics of straight-and headed-end, ribbed-surface, GFRP bars embedded in high-strength concrete. *Constr Build Mater* 83:283–298



36. Elsayed TA, Eldaly A, El-Hefnawy A, Ghanem G (2011) Behaviour of concrete beams reinforced with hybrid fiber reinforced bars. *Adv Compos Mater* 20(3):245–259
37. Shakiba M, Oskouei AV, Karamloo M, Doostmohamadi A (2021) Effect of mat anchorage on flexural bonding strength between concrete and sand coated GFRP bars. *Compos Struct* 273:114339
38. Ashrafi H, Bazli M, Oskouei AV (2017) Enhancement of bond characteristics of ribbed-surface GFRP bars with concrete by using carbon fiber mat anchorage. *Constr Build Mater* 134:507–519
39. Ahmed EA, El-Sayed AK, El-Salakawy E, Benmokrane B (2010) Bend strength of FRP stirrups: comparison and evaluation of testing methods. *J Compos Constr* 14(1):3–10
40. Saleh N, Ashour A, Lam D, Sheehan T (2019) Experimental investigation of bond behaviour of two common GFRP bar types in high-strength concrete. *Constr Build Mater* 201:610–622
41. Basaran B, Kalkan I (2020) Investigation on variables affecting bond strength between FRP reinforcing bar and concrete by modified hinged beam tests. *Compos Struct* 242:112185
42. Rosa I, Firmo J, Correia J, Barros J (2019) Bond behaviour of sand coated GFRP bars to concrete at elevated temperature—definition of bond vs. slip relations. *Compos Part B Eng* 160:329–340
43. Saleh N, Ashour A, Sheehan T (2019) Bond between glass fibre reinforced polymer bars and high-strength concrete. Elsevier, Structures, pp 139–153
44. Taha A, Alnahhal W, Alnuaimi N (2020) Bond durability of basalt FRP bars to fiber reinforced concrete in a saline environment. *Compos Struct* 243:112277
45. Dong Z-Q, Wu G, Zhao X-L, Lian J-L (2018) Long-term bond durability of fiber-reinforced polymer bars embedded in seawater sea-sand concrete under ocean environments. *J Compos Constr* 22(5):04018042
46. Lu Z, Su L, Lai J, Xie J, Yuan B (2021) Bond durability of BFRP bars embedded in concrete with fly ash in aggressive environments. *Compos Struct* 271:114121
47. Ahmed A, Guo S, Zhang Z, Shi C, Zhu D (2020) A review on durability of fiber reinforced polymer (FRP) bars reinforced seawater sea sand concrete. *Constr Build Mater* 256:119484
48. Wang L, Mao Y, Lv H, Chen S, Li W (2018) Bond properties between FRP bars and coral concrete under seawater conditions at 30, 60, and 80 C. *Constr Build Mater* 162:442–449
49. Kazemi H, Yekrangnia M, Shakiba M, Bazli M, Oskouei AV (2022) Bond-slip behaviour between GFRP/steel bars and seawater concrete after exposure to environmental conditions. *Eng Struct* 268:114796
50. Davalos JF, Chen Y, Ray I (2008) Effect of FRP bar degradation on interface bond with high strength concrete. *Cement Concr Compos* 30(8):722–730
51. Robert M, Benmokrane B (2010) Effect of aging on bond of GFRP bars embedded in concrete. *Cement Concr Compos* 32(6):461–467
52. Ruiz Empananza A, De Caso F, Basalo Y, Kampmann R, AdarragaUsabiaga I (2018) Evaluation of the bond-to-concrete properties of GFRP rebars in marine environments. *Infrastructures* 3(4):44
53. Hassan M, Benmokrane B, ElSafty A, Fam A (2016) Bond durability of basalt-fiber-reinforced-polymer (BFRP) bars embedded in concrete in aggressive environments. *Compos B Eng* 106:262–272
54. El Refai A, Abed F, Altalmas A (2015) Bond durability of basalt fiber-reinforced polymer bars embedded in concrete under direct pullout conditions. *J Compos Constr* 19(5):04014078
55. Altalmas A, El Refai A, Abed F (2015) Bond degradation of basalt fiber-reinforced polymer (BFRP) bars exposed to accelerated aging conditions. *Constr Build Mater* 81:162–171
56. Yang Y, Li Z, Zhang T, Wei J, Yu Q (2017) Bond-slip behavior of basalt fiber reinforced polymer bar in concrete subjected to simulated marine environment: effects of BFRP bar size, corrosion age, and concrete strength. *Int J Polym Sci*. <https://doi.org/10.1155/2017/5156189>
57. Yan F, Lin Z (2017) Bond durability assessment and long-term degradation prediction for GFRP bars to fiber-reinforced concrete under saline solutions. *Compos Struct* 161:393–406
58. Belarbi A, Wang H (2012) Bond durability of FRP bars embedded in fiber-reinforced concrete. *J Compos Constr* 16(4):371–380
59. Yan F, Lin Z, Zhang D, Gao Z, Li M (2017) Experimental study on bond durability of glass fiber reinforced polymer bars in concrete exposed to harsh environmental agents: Freeze-thaw cycles and alkaline-saline solution. *Compos B Eng* 116:406–421
60. Taha A, Alnahhal W (2021) Bond durability and service life prediction of BFRP bars to steel FRC under aggressive environmental conditions. *Compos Struct* 269:114034
61. Zhou J, Chen X, Chen S (2011) Durability and service life prediction of GFRP bars embedded in concrete under acid environment. *Nucl Eng Des* 241(10):4095–4102
62. Zhou J, Chen X, Chen S (2012) Effect of different environments on bond strength of glass fiber-reinforced polymer and steel reinforcing bars. *KSCE J Civ Eng* 16(6):994–1002
63. Yang S, Yang C, Huang M, Liu Y, Jiang J, Fan G (2018) Study on bond performance between FRP bars and seawater coral aggregate concrete. *Constr Build Mater* 173:272–288
64. Bazli M, Ashrafi H, Oskouei AV (2017) Experiments and probabilistic models of bond strength between GFRP bar and different types of concrete under aggressive environments. *Constr Build Mater* 148:429–443
65. Raman R, Guo F, Al-Saadi S, Zhao X-L, Jones R (2020) Understanding fibre-matrix degradation of FRP composites for advanced civil engineering applications: an overview. *Corros Mater Degrad* 1(1):27–41
66. Soles CL, Chang FT, Bolan BA, Hristov HA, Gidley DW, Yee AF (1998) Contributions of the nanovoid structure to the moisture absorption properties of epoxy resins. *J Polym Sci Part B Polym Phys* 36(17):3035–3048
67. ACI 440.3R-12 (2012) Guide test methods for fiber-reinforced polymer (FRP) composites for reinforcing or strengthening concrete and masonry structures. Structural Building Code, American Concrete Institute, Farmington Hills, MI, USA
68. Arias JPM, Vazquez A, Escobar MM (2012) Use of sand coating to improve bonding between GFRP bars and concrete. *J Compos Mater* 46(18):2271–2278



69. Aslani F (2019) Residual bond between concrete and reinforcing GFRP rebars at elevated temperatures. *Proc Inst Civil Eng Struct Build* 172(2):127–140
70. Ceroni F, Cosenza E, Gaetano M, Pecce M (2006) Durability issues of FRP rebars in reinforced concrete members. *Cement Concr Compos* 28(10):857–868
71. Huang P, Bao Y, Yao Y (2005) Influence of HCl corrosion on the mechanical properties of concrete. *Cem Concr Res* 35(3):584–589
72. Mohammed TU, Hamada H, Yamaji T (2004) Performance of seawater-mixed concrete in the tidal environment. *Cem Concr Res* 34(4):593–601
73. Fam A, Boles R, Robert M (2016) Durability in a salt solution of pultruded composite materials used in structural sections for bridge deck applications. *J Bridg Eng* 21(1):04015032
74. Kafodya I, Xian G, Li H (2015) Durability study of pultruded CFRP plates immersed in water and seawater under sustained bending: water uptake and effects on the mechanical properties. *Compos B Eng* 70:138–148

**Publisher's Note** Springer Nature remains neutral with regard to jurisdictional claims in published maps and institutional affiliations.

